Journal of Coordination Chemistry, 2014
Vol. 67, No. 7, 1265–1278, http://dx.doi.org/10.1080/00958972.2014.910597

Synthesis, structure, and urease inhibitory activities of three binuclear copper(II) complexes with protocatechuic acid derivative

GUI-HUA SHENG†‡, QUAN-CHENG ZHOU†§, JUAN SUN†‡, XIAO-SHAN CHENG¶, SHAO-SONG QIAN†, CHUN-YANG ZHANG†, ZHONG-LU YOU*¶ and HAI-LIANG ZHU*†‡

†State Key Laboratory of Pharmaceutical Biotechnology, Nanjing University, Nanjing, PR China
‡School of Life Sciences, Shandong University of Technology, Zibo, PR China
§School of Agricultural Engineering and Food Science, Shandong University of Technology, Zibo, PR China
¶Department of Chemistry and Chemical Engineering, Liaoning Normal University, Dalian, PR China

(*Received 21 February 2013; accepted 11 March 2014*)

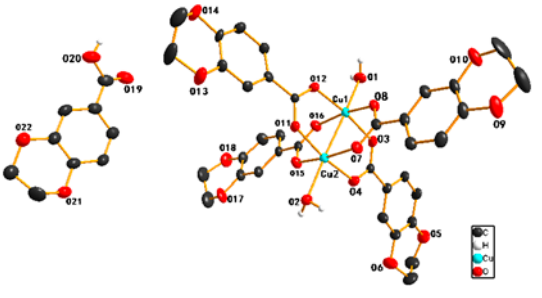

Three Cu(II) complexes, $[Cu^{II}_2(L_1)_4(L_2)_2]$ (**1**), $[Cu^{II}_2(L_1)_4(H_2O)_2]\cdot HL$ (**2**), and $[Cu^{II}_2(L_1)_3(L_3)_2]ClO_4$ (**3**), with a ligand derived from protocatechuic acid ($HL_1 = C_9H_8O_4$=2,3-dihydrobenzo[*b*][1,4]-dioxine-6-carboxylic acid, $L_2 = C_7H_9N$=*o*-toluidine, $L_3 = C_6H_{16}N_2$=N,N-diethylethylenediamine) were synthesized and characterized by C, H, and N elemental analysis and single-crystal X-ray diffraction, which revealed that the three complexes have similar binuclear structures. Complexes **1** and **3** crystallized in triclinic space group *P-1* and **2** in orthorhombic space group $P2_12_12_1$. The urease inhibitory activities of the three complexes were tested. All three complexes showed strong inhibitory activity against *jack bean* urease with an IC_{50} value of 6.8, 5.5, and 3.5 μM compared with the acetohydroxamic acid ($IC_{50} = 7.5$ μM), which was a positive control.

Keywords: Copper(II) complex; Crystal structure; Urease inhibitors; Protocatechuic acid

*Corresponding authors. Email: youzhonglu@lnnu.edu.cn (Z.-L. You); zhuhl@nju.edu.cn (H.-L. Zhu)
G.-H. Sheng and Q.-C. Zhou are contributed equally to this paper.

1. Introduction

Urease (urea amidohydrolase; E.C.3.5.1.5) is a nickel-containing metalloenzyme that rapidly catalyzes the hydrolysis of urea to ammonia and carbamate [1, 2]. Urease is widely distributed in a variety of algae, bacteria, fungi and plants. The reaction catalyzed by urease may cause an accumulation of ammonia and accompanying pH elevation, which has negative implications in medicine and agriculture [3–6]. Urease in *Helicobacter pylori* is accepted as a major cause of peptic ulcers [2]. *H. pylori* is characterized by very high urease activity which may act as a virulence or survival factor. Urease inhibitors could counteract these negative effects through control of the activity of urease, so urease inhibitors are very important in treatment of infections caused by urease-producing bacteria [7]. Current efforts are focused on the discovery of urease inhibitors against *H. pylori* urease. Therefore, urease inhibitors have recently attracted attention as potential new anti-ulcer drugs. Urease inhibitors can be broadly classified into two fields: (1) organic compounds, such as acetohydroxamic acid, humic acid, and 1,4-benzoquinone [8–10] and (2) metal ions, such as Cu^{2+}, Zn^{2+}, Pd^{2+}, and Cd^{2+} [11, 12]. Some metal complexes have been reported to show urease inhibitory activities [13–17]. Protocatechuic acid (3,4-dihydroxybenzoic acid) is a simple phenolic compound widely distributed in nature. It is detected in almost all plants and is one of the biologically active components of some medicinal plants, including those used in natural medicine. It is reported that protocatechuic acid has antioxidant, anti-radical activity, and chemopreventive ability in chemically induced carcinogenesis [18–20]. Some complexes with protocatechuic acid and its derivatives as ligands have been reported [21, 22]. In this article, we report the synthesis of a protocatechuic acid derivative and synthesized three new binuclear copper(II) complexes with the derivative. The structure and urease inhibitory activity of these complexes were evaluated.

2. Experimental

2.1. *General methods and materials*

Unless otherwise stated all solvents were of reagent grade and purchased commercially. All chemicals were also commercially available and used without purification. Elemental analyses were performed on a Perkin-Elmer 240C elemental analyzer.

2.2. *Synthesis of 2,3-dihydrobenzo[b][1,4]dioxine-6-carboxylic acid*

The protocatechuic acid derivative 2,3-dihydrobenzo[*b*][1,4]dioxine-6-carboxylic acid ($C_9H_8O_4$, HL_1) was synthesized with protocatechuic acid (3,4-dihydroxybenzoic acid) and 1,2-dibromoethane (scheme 1). Yield 81%. M.p. 133–137 °C. Anal. Calcd for $C_9H_8O_4$: C, 60.00; H, 4.48%. Found: C, 60.02; H, 4.46%. The synthesis method is different from that reported in the literatures which synthesized the compound with 2,3-dihydrobenzo[*b*][1,4] dioxine or 2,3-dihydrobenzo[*b*][1,4]dioxine-6-carbaldehyde [23, 24]. Three complexes were synthesized by the reaction of HL_1 with the corresponding metal salts (scheme 2) in a solution of aqueous ethanol; *o*-toluidine (C_7H_9N, L_2) and N,N-diethylethylenediamine ($C_6H_{16}N_2$, L_3) were added to the solutions for **1** and **3**, respectively.

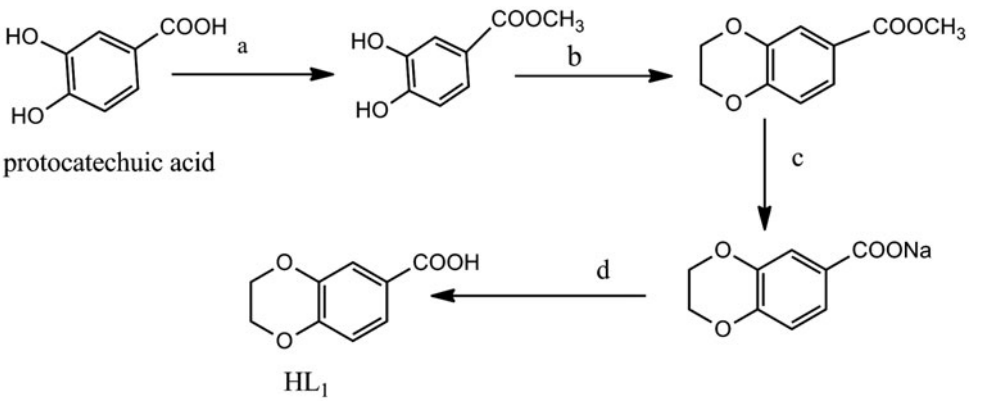

Scheme 1. Synthesis of HL1(2,3-dihydrobenzo[b][1,4]dioxine-6-carboxylic acid). Reagents and conditions: (a) MeOH, H_2SO_4, reflux, 8 h; (b) $Br(CH_2)_2Br$, acetone, reflux, 24 h; (c) NaOH, H_2O, reflux, 5 h; (d) HCl.

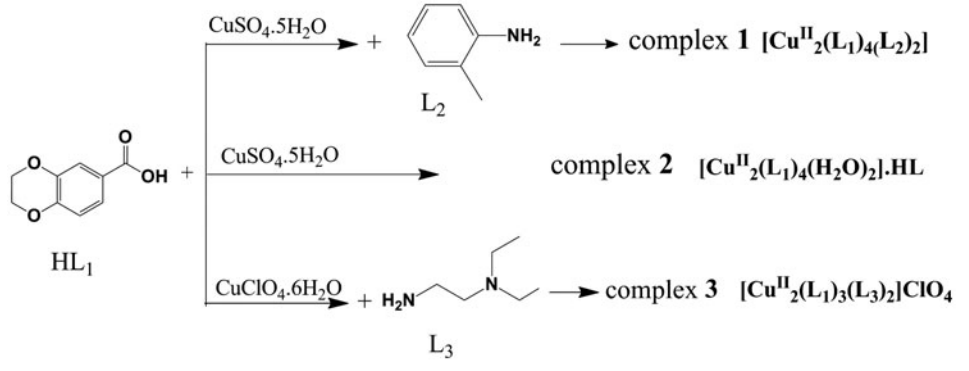

Scheme 2. Synthesis of **1**–**3**.

2.3. *Synthesis of 1*

An ethanol solution (2 mL) of HL_1 (0.2 mM, 0.036 g) and $CuSO_4{\cdot}5H_2O$ (0.1 mM, 0.0159 g) was added to H_2O solution (4 mL) of *o*-toluidine (0.1 mM, 0.0107 g). The mixture was stirred for 30 min at room temperature to give a green clear solution. After keeping the solution in air for five days, green block-shaped single crystals of **1** suitable for structure determination were obtained on slow evaporation of the solvent. Crystals were isolated by filtration and washed with cold ethanol and then dried in air. Yield 81%. Anal. Calcd for $C_{50}H_{46}Cu_2N_2O_{16}$: C, 56.76; H, 4.38; N, 2.65%. Found: C, 56.63; H, 4.36; N, 2.64%.

2.4. *Synthesis of 2*

An ethanol solution (2 mL) of HL_1 (0.2 mM, 0.036 g) was added to a H_2O solution (4 mL) of $CuSO_4{\cdot}5H_2O$ (0.1 mM, 0.0159 g). The mixture was stirred for 30 min at room temperature to give a green clear solution. After keeping the solution in air for five days, green block-shaped single crystals of **2** suitable for structure determination were obtained

on slow evaporation of the solvent. Crystals were isolated by filtration and washed with cold ethanol and then dried in air. Yield 75%. Anal. Calcd for $C_{45}H_{40}O_{22}Cu_2$: C, 50.99; H, 3.80%. Found: C, 50.80; H, 3.65%.

2.5. *Synthesis of 3*

HL_1 (0.2 mM, 0.036 g) and $Cu(ClO_4)_2 \cdot 6H_2O$ (0.1 mM, 0.037 g) were added to 6 mL ethanol and H_2O mixture (v : v = 2 : 4). The mixture was stirred for 30 min; concentrated ammonia was added to the mixture to promote dissolution to give a blue clear solution. N,N-Diethylethylenediamine (0.1 mM, 0.0116 g) was added to the solution. The solution was filtered; after keeping the filtrate in air for 20 days, blue block-shaped single crystals of **3** suitable for structure determination were obtained on slow evaporation of the solvent. Crystals were isolated by filtration and washed with cold ethanol and then dried in air. Yield 83%. Anal. Calcd for $C_{39}H_{53}N_4O_{16}ClCu_2$: C, 47.01; H, 5.36; N, 5.62%. Found: C, 46.92; H, 5.32; N, 5.65%.

2.6. *Crystal structure determination*

X-ray diffraction intensities were collected using a Bruker SMART APEX-II CCD area detector equipped with graphite-monochromated Mo Kα radiation ($\lambda = 0.71073$ Å). Absorption correction was applied by SADABS [25]. The structure was solved by direct

Table 1. Crystal and experimental data for **1–3**.

	Complex **1**	Complex **2**	Complex **3**
Molecular formula	$C_{50}H_{46}Cu_2N_2O_{16}$	$C_{45}H_{40}O_{22}Cu_2$	$C_{39}H_{53}N_4O_{16}ClCu_2$
Molecular weight	1057.99	1059.87	996.40
Temperature (K)	293	298	293
Radiation λ	Mo Kα (0.7107 Å)	Mo Kα (0.7107 Å)	Mo Kα (0.7107 Å)
Crystal system	Triclinic	Orthorhombic	Triclinic
Space group	*P-1*	$P2_12_12_1$	*P-1*
a (Å)	7.6688(5)	12.5828(13)	9.9262(6)
b (Å)	12.4183(9)	13.5193(14)	15.0558(9)
c (Å)	13.8603(9)	25.605(3)	16.4227(11)
α (°)	68.489(2)	90.00	94.843(2)
β (°)	78.691(2)	90.00	103.908(2)
γ (°)	72.285(2)	90.00	108.410(2)
V (Å^3)	1164.46(14)	4355.6(8)	2225.9(2)
Z	1	4	2
D_{Calcd} (g cm^{-3})	1.509	1.616	1.487
Crystal size (mm^3)	0.30 × 0.20 × 0.22	0.24 × 0.22 × 0.16	0.26 × 0.25 × 0.19
F (0 0 0)	546	2176	1036
θ Range (°)	2.78–26.49	2.19–27.14	2.3–25.8
Reflections collected/unique	11,287/4787 [$R_{int} = 0.0152$]	37,830/9604 [$R_{int} = 0.1016$]	21,169/8456 [$R_{int} = 0.0254$]
Refns obs. $I > 2\sigma(I)$	4353	6270	6902
Goodness of fit on F^2	1.071	1.011	1.036
Data/parameters/restraints	4787/335/0	9604/668/69	8456/593/34
Largest diff. peak and hole (e Å^{-3})	0.257 and −0.374	1.249 and −1.226	1.194 and −0.773
R_1, wR_2 [$I > 2\sigma(I)$][a]	0.0304, 0.0773	0.0688, 0.1648	0.0496, 0.1355
R_1, wR_2 (all data)[a]	0.0357, 0.0805	0.1270, 0.1968	0.0629, 0.1463

[a] $R_1 = F_o - F_c/F_o$, $wR_2 = \left[\sum w(F_o^2 - F_c^2)/\sum w(F_o^2)^2\right]^{1/2}$.

methods and refined on F^2 by full-matrix least-squares using Bruker's SHELXTL-97 program [26]. All non-hydrogen atoms were refined anisotropically. The water hydrogens were located from a difference Fourier map and refined isotropically, with O–H and H···H distances restrained to 0.85(1) and 1.35(2) Å, respectively. The remaining hydrogens were placed in calculated positions and constrained to ride on their parent. There are 69 and 34 restraints used to deal with the structure disorder during the refinement of **2** and **3**, respectively. The details of the crystallographic data are summarized in table 1. Selected bond lengths and angles are listed in table 2. Geometrical parameters for hydrogen bonds are shown in table 3.

Table 2. Selected distances (Å) and angles (°) for **1–3**.

Complex **1** (#1: $-x+1, -y+1, -z$)			
Cu(1)–O(1)	1.9769(13)	Cu(1)–O(5)	1.9608(13)
Cu(1)–O(2)$^{\#1}$	1.9861(14)	Cu(1)–N(1)	2.2271(16)
Cu(1)–O(6)	1.9509(13)	Cu1…Cu1$^{\#1}$	2.6377(4)
O5–Cu1–O6	168.32(6)	O2–Cu1–N1$^{\#1}$	90.32(6)
O6–Cu1–O1	91.16(6)	O5–Cu1–O1	87.91(6)
O6–Cu1–O2$^{\#1}$	88.99(6)	O5–Cu1–O2$^{\#1}$	89.59(6)
O1–Cu1–O2$^{\#1}$	168.33(5)	O6–Cu1–N1	97.05(6)
O5–Cu1–N1	94.56(6)	O1–Cu1–N1	101.24(6)
Complex **2**			
Cu1–O8	1.958(5)	Cu2–O15	1.936(5)
Cu1–O12	1.977(4)	Cu2–O4	1.955(4)
Cu1–O1	2.162(4)	Cu2–O2	2.189(4)
Cu1–O16	1.963(5)	Cu2–O7	1.945(5)
Cu1–O3	1.973(4)	Cu2–O11	1.987(4)
Cu1…Cu2	2.5789(10)		
O8–Cu1–O12	89.9(2)	O15–Cu2–O11	89.1(2)
O8–Cu1–O3	89.9(2)	O4–Cu2–O11	168.83(19)
O12–Cu1–O3	171.2(2)	O7–Cu2–O2	93.86(19)
O16–Cu1–O1	93.2(2)	O11–Cu2–O2	97.04(18)
O3–Cu1–O1	93.7(2)	O15–Cu2–O4	89.3(2)
O16–Cu1–O12	89.8(2)	O7–Cu2–O4	89.7(2)
O16–Cu1–O3	88.5(2)	O7–Cu2–O11	90.3(2)
O8–Cu1–O1	99.1(2)	O15–Cu2–O2	94.56(19)
O12–Cu1–O1	94.98(19)	O4–Cu2–O2	94.11(19)
O8–Cu1–O16	167.7(2)	O15–Cu2–O7	171.6(2)
Complex **3**			
Cu1–O9	1.937(2)	Cu2–O13	1.974(3)
Cu1–O14	2.032(2)	Cu2–O10	1.954(2)
Cu1–N2	2.198(3)	Cu2–N4	2.272(3)
Cu1–N1	1.989(3)	Cu2–O6	1.962(2)
Cu1–O5	2.035 (2)	Cu2–N3	2.011(3)
Cu1…Cu2	2.9069(6)		
O9–Cu1–N1	177.54(13)	O10–Cu2–O6	90.53(12)
N1–Cu1–O14	87.06(13)	O10–Cu2–O13	90.13(11)
N1–Cu1–O5	89.44(13)	O10–Cu2–N3	175.67(13)
O9–Cu1–N2	94.75(12)	O13–Cu2–N3	87.65(14)
O14–Cu1–N2	105.75(13)	O6–Cu2–N4	100.11(12)
O9–Cu1–O14	91.95(11)	N3–Cu2–N4	84.27(13)
O9–Cu1–O5	92.53(11)	O6–Cu2–O13	168.04(11)
O14–Cu1–O5	150.06 (11)	O6–Cu2–N3	90.87(14)
N1–Cu1–N2	83.36 (14)	O10–Cu2–N4	99.51(11)
O5–Cu1–N2	103.35 (13)	O13–Cu2–N4	91.56(11)

Table 3. Geometrical parameters for hydrogen bonds.

Hydrogen bonds	Symmetry code	*D*–H (Å)	H···*A* (Å)	*D*···*A* (Å)	*D*–H···*A* (°)
Complex **1**					
N1–H1B…O2	[*x* + 1, *y*, *z*]	0.90	2.59	3.353(4)	143.44
Complex **2**					
O1–H1A…O21	[−*x* + 1, *y* − 1/2, −*z* + 1/2]	0.850	2.073	2.802	143.50
O2–H2A…O12	[−*x*, *y* + 1/2, −*z* + 1/2]	0.820	2.231	2.909	140.25
O20–H20…O14	[*x* + 1/2, −*y* + 1/2, −*z* + 1]	0.820	1.916	2.699	159.22
O2–H2B…O19	[−*x* + 1, *y* + 1/2, −*z* + 1/2]	0.849	2.040	2.838	156.38
O1–H1B…O2	[−*x*, *y* − 1/2, −*z* + 1/2]	0.846	2.266	2.985	142.96
O1–H1B…O11	[−*x*, *y* − 1/2, −*z* + 1/2]	0.846	2.567	3.127	124.67
Complex **3**					
N3–H3B…O4		0.896(10)	2.28(3)	3.105(5)	154(6)
N3–H3A…O2	[−*x* + 1, −*y* + 1, −*z* + 1]	0.896(11)	2.324(19)	3.210(7)	170(7)
N1–H1B…O2	[−*x* + 1, −*y* + 1, −*z* + 1]	0.895(10)	2.214(18)	3.099(7)	170(6)
N1–H1A…O3		0.896(10)	2.43(4)	3.233(7)	150(6)
N1–H1A…O4		0.896(10)	2.42(4)	3.249(6)	154(6)

2.7. *Measurement of inhibitory activity against jack bean urease*

Jack bean urease was purchased from Sigma Aldrich Co. (St. Louis, MO, USA). The measurement of urease was carried out according to the literature [27, 28]. Generally, the assay mixture, containing 25 µL of *jack bean* urease (10 kU/L) and 25 µL of the tested samples (complexes, ligands, and metal salts) of various concentrations [dissolved in solution of DMSO : H_2O = 1 : 1 (v : v)], was preincubated for 1 h at 37 °C in a 96-well assay plate. After preincubation, 0.2 mL of 100 mM phosphate buffer at pH 6.8 containing 500 mM urea and 0.002% phenol red were added and incubated at 37 °C. The reaction time was measured by micro-plate reader (570 nm), which was required to produce enough ammonium carbonate to raise the pH of a phosphate buffer from 6.8 to 7.7, the end-point being determined by the color of phenol red indicator.

3. Results and discussion

3.1. *Crystal structure description of the complexes*

Single-crystal X-ray diffraction reveals that $[Cu^{II}_2(L_1)_4(L_2)_2]$ (**1**), $[Cu^{II}_2(L_1)_4(H_2O)_2]\cdot HL$ (**2**), and $[Cu^{II}_2(L_1)_3(L_3)_2]ClO_4$ (**3**) have similar binuclear structures. There are two copper ions in each complex, linked by four (for **1** and **2**) or three (for **3**) bridging bidentate L_1. The carboxylate bridged Cu…Cu distances of **1–3** are 2.6377(4), 2.5789(10), and 2.9069 (6) Å, respectively, comparable to those reported in similar binuclear carboxylate copper complexes [29–32].

3.1.1. Structure of 1. Complex **1** crystallizes in the triclinic space group *P-1*. Perspective views of the crystal structure of **1** are shown in figure 1. Each molecule consists of two copper ions, four 2,3-dihydrobenzo[*b*][1,4]dioxine-6-carboxylic acid (L_1) anions, and two

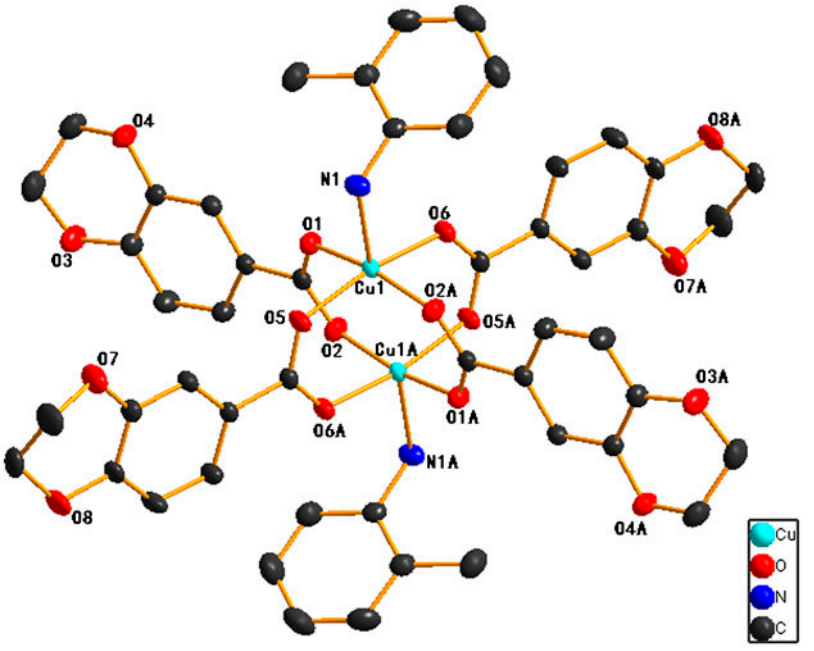

Figure 1. A perspective view of **1** with atom-labeling scheme (symmetry code: A $-x+1, -y+1, -z$). The thermal ellipsoids are drawn at the 30% probability level (hydrogens are omitted for clarity).

o-toluidine (L_2) molecules. Each copper is five coordinate with four oxygens of L_1 and one N of L_2 in square–pyramidal arrangement ($\tau = 0.0002$ for Cu1 and Cu1A) [33], thus forming a $[CuO_4N_1]$ chromophore. Two copper ions are linked by four bridging bidentate carboxylic groups of four L_1. Four oxygens of four L_1 anions form the basal plane and one N of L_2 is in the axial position. The in-plane Cu–O bond distances average 1.97 Å and axial Cu–N bond distance is 2.23 Å, in the normal ranges (figure 1 and table 2) [34]. In the crystal, intermolecular N1–H1B…O2 $[x+1, y, z]$ hydrogen bonds serve as bridges to link adjacent molecules into 1-D chains along the *a* axis (figure 2 and table 3).

3.1.2. Structure of 2. Complex **2** is in the orthorhombic space group $P2_12_12_1$. Perspective views of the crystal structure of **2** are shown in figure 3. Each complex consists of one $[Cu^{II}_2(L_1)_4(H_2O)_2]$ and one uncoordinated HL. In each $[Cu^{II}_2(L_1)_4(H_2O)_2]$, there are two copper ions, four L_1 anions, and two H_2O molecules. Each copper is five coordinate with four oxygens from L_1 and one H_2O in the distorted square–pyramidal arrangement ($\tau = 0.058$ for Cu1 and 0.046 for Cu2) [33], forming a $[CuO_5]$ chromophore. Two copper ions are linked by four bridging bidentate carboxylates of L_1. Four L_1 anions form the basal plane and H_2O is axial. The in-plane Cu–O bond distances average 1.96 Å and axial Cu–O bond distance is 2.18 Å, in the normal ranges [34]. O1–Cu1–O8 and O1–Cu1–O16 bond angles (99.1(2) and 93.2(2) Å, respectively) reflect the distorted square–pyramidal geometry surrounding Cu1. O11–Cu2–O2 and O7–Cu2–O2 bond angles (97.04(18) and 93.86(19) Å, respectively) reflect the distorted square–pyramidal geometry surrounding Cu2 (figure 3 and table 2). The binuclear units form a 1-D chain-like structure extended along the

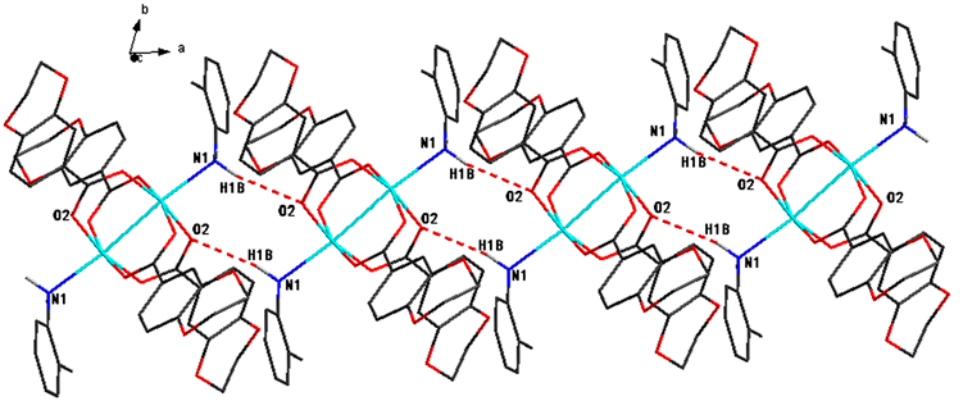

Figure 2. View of the hydrogen bond-driven 1-D chain of **1** running along the *a* axis. Hydrogen bonds are shown as dashed lines.

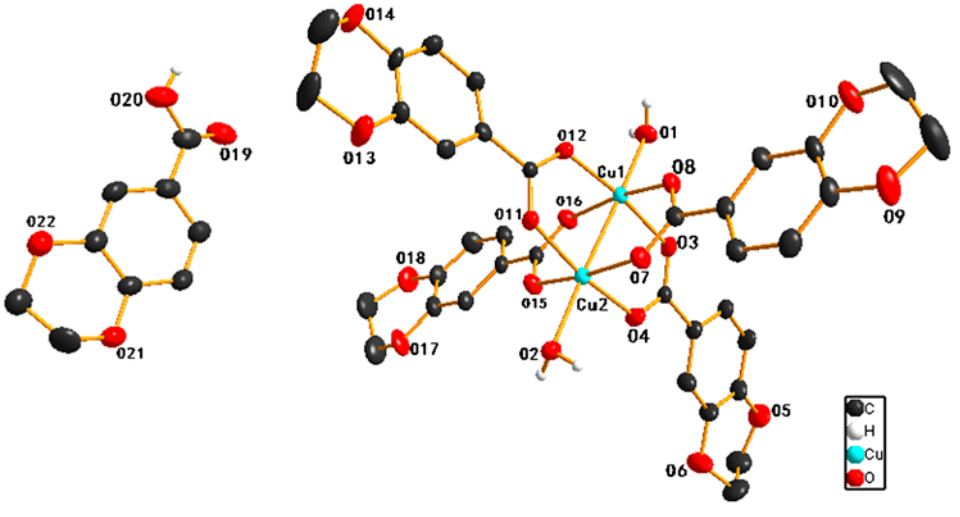

Figure 3. A perspective view of **2** with the atom-labeling scheme. The thermal ellipsoids are drawn at the 30% probability level (hydrogens are omitted for clarity).

crystallographic *b* axis via five hydrogen bonds: O1–H1A…O21 ($-x+1$, $y-1/2$, $-z+1/2$; 2.802 Å), O1–H1B…O2 ($-x$, $y-1/2$, $-z+1/2$; 2.985 Å), O1–H1B…O11 ($-x$, $y-1/2$, $-z+1/2$; 3.127 Å), O2–H2A…O12 ($-x$, $y+1/2$, $-z+1/2$; 2.909 Å), O2–H2B…O19 ($-x+1$, $y+1/2$, $-z+1/2$; 2.838 Å). One free HL_1 is linked with two $[Cu^{II}_2(L_1)_4(H_2O)_2]$ and involved in the formation of the 1-D chain along the *b* axis (figure 4 and table 3). Free HL_1 molecules link the chains (running along the *b* axis, highlighted by different color) into a 2-D network (figure 5 and table 3) via three intermolecular H bonds: O1–H1A…O21 ($-x+1$, $y+1/2$, $-z+0.5$), O2–H2B…O19 ($-x+1$, $y-1/2$, $-z+0.5$), and O20–H20…O14 ($x+1/2$, $-y+1/2$, $-z+1$). In free HL_1, O19, and O21 are H acceptors linked with one 1-D chain which along the *b* axis and O20 is an H donor to O14 of another 1-D chain linking

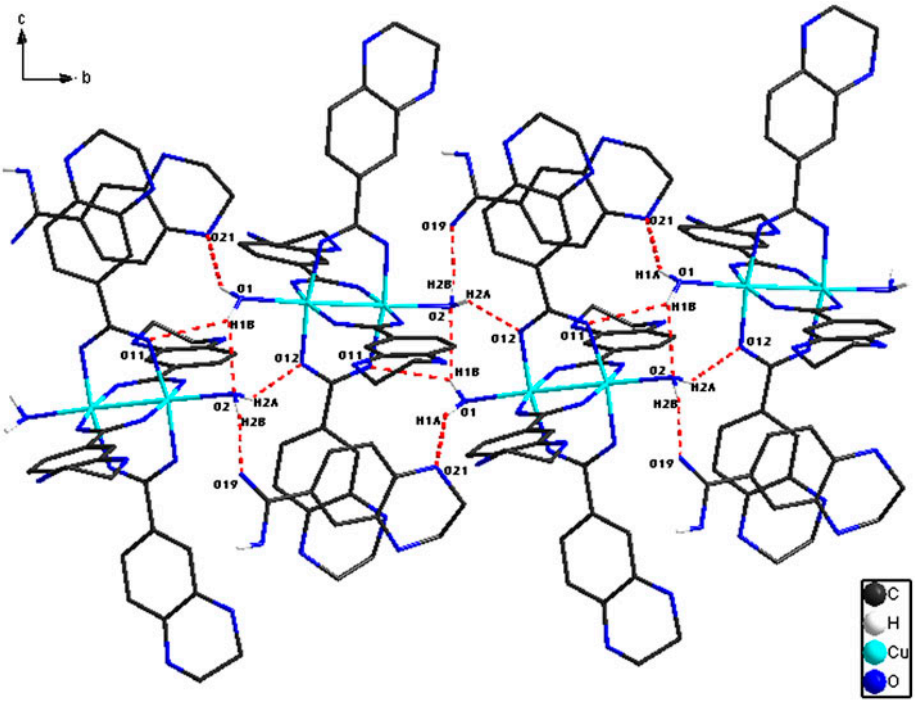

Figure 4. View of the hydrogen bond-driven 1-D chain of **2** running along the *b* axis. Hydrogen bonds are shown as dashed lines.

adjacent 1-D chains into the 2-D network. Free HL_1 also links 2-D structures into a 3-D network in the same way via the aforementioned three intermolecular H bonds (figure 6 and table 3).

3.1.3. Structure of 3. Complex **3** is in the triclinic space group *P-1*. Perspective views of the crystal structure of **3** are shown in figure 7. Each complex consists of one $[Cu^{II}_2(L_1)_3(L_3)_2]^+$ and one ClO_4^-. In each $[Cu^{II}_2(L_1)_3(L_3)_2]^+$, there are two copper ions, three L_1, two N,N-diethylethylenediamine (L_3), and one perchlorate. Each copper is five coordinate with three oxygens of L_1 and two nitrogens of L_3 in distorted square–pyramidal arrangement ($\tau = 0.46$ for Cu1 and 0.13 for Cu2), thus forming a $[CuO_3N_2]$ chromophore. Two copper ions are linked by three bridging bidentate carboxylates. Three oxygens of three L_1 and one nitrogen from L_3 form the basal plane, and the other N of L_3 is in the axial position. Cu–O and Cu–N bond distances are in the normal range [34]. N2–Cu1–O14 and N1–Cu1–N2 bond angles (105.75(13) and 83.36(14) Å, respectively) reflect the distorted square pyramidal geometry surrounding Cu1. O6–Cu2–N4 and N3–Cu2–N4 bond angles (100.11(12) and 84.27(13) Å, respectively) reflect the distorted square–pyramidal geometry surrounding Cu2. Two complex molecules are linked forming a dimer by intramolecular and intermolecular hydrogen bonds (figure 8 and table 3): N3–H3B…O4 (3.105(5) Å), N1–H1A…O3 (3.233(7) Å), N1–H1A…O4 (3.249(6) Å), N3–H3A…O2 [$-x+1$, $-y+1$, $-z+1$] (3.210(7) Å), N1–H1B…O2 [$-x+1$, $-y+1$, $-z+1$] (3.099(7) Å).

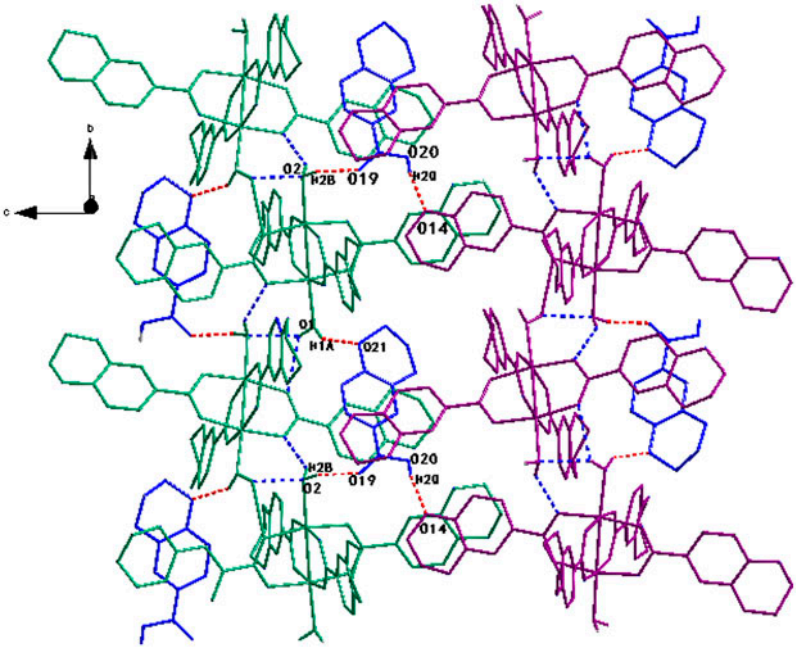

Figure 5. View of free HL_1 connecting adjacent 1-D chains (running along the *b* axis, highlighted by different color) into a 2-D network. Hydrogen bonds are shown as dashed lines.

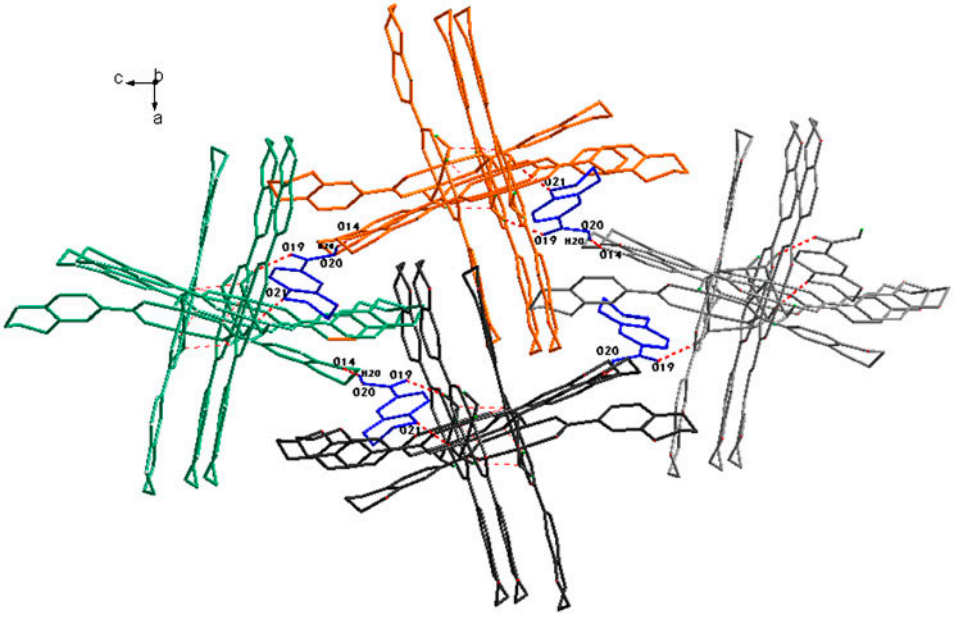

Figure 6. View of free HL_1 connecting 1-D chains (running along the *b* axis, highlighted by different color) into a 3-D network. Hydrogen bonds are shown as dashed lines.

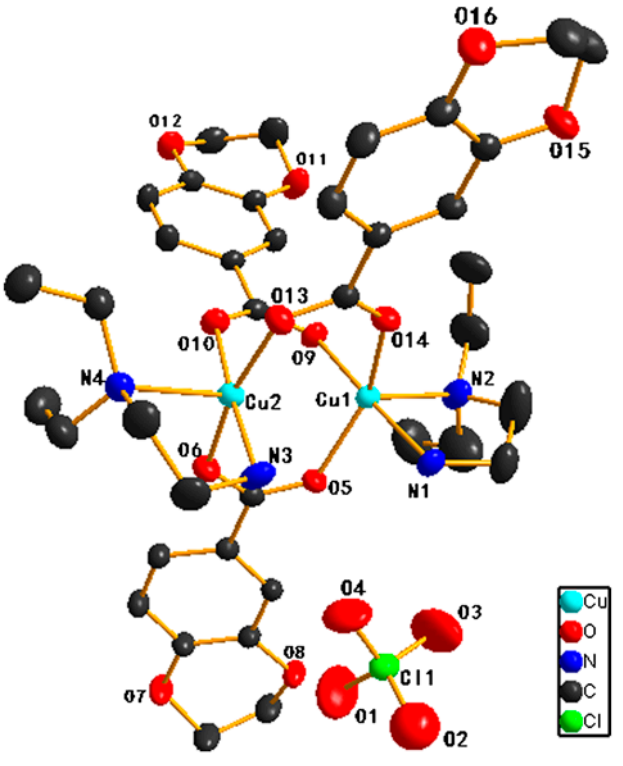

Figure 7. A perspective view of **3** with the atom-labeling scheme. The thermal ellipsoids are drawn at the 30% probability level (hydrogens are omitted for clarity).

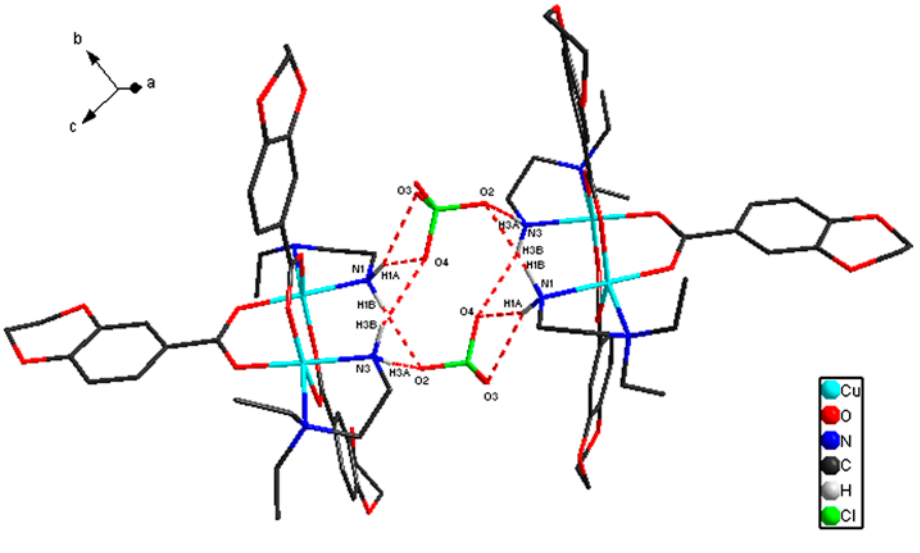

Figure 8. View of dimer of **3** via hydrogen bonds (shown as dashed lines).

Table 4. Inhibition of urease by the tested materials.

Tested materials	IC_{50} (μm)
HL_1	>10
L_2	>10
L_3	>10
$CuSO_4 \cdot 5H_2O$	>10
Complex **1**: $[Cu^{II}_2(L_1)_4(L_2)_2]$	6.8 ± 0.4
Complex **2**: $[Cu^{II}_2(L_1)_4(H_2O)_2] \cdot HL$	5.5 ± 0.4
Complex **3**: $[Cu^{II}_2(L_1)_3(L_3)_2]ClO_4$	3.5 ± 0.3
Acetohydroxamic acid	7.5 ± 0.6

3.2. *IR and UV–vis spectra*

Infrared spectra of HL_1 and the three complexes provide information about the metal–ligand bonding. For HL_1, the strong absorption band at 1686 cm^{-1} is assigned to C=O(Ar–COOH) stretch and the broad absorptions at 2500–2663 cm^{-1} are assigned to O–H(Ar–COOH) stretch. These two absorptions are absent in the three complexes, indicating complete deprotonation and coordination of L_1 in the complexes. The weak and moderate bands around 3400 cm^{-1} of **2** are assigned to O–H vibrations of water. The absorptions at 3200–3340 cm^{-1} of **1** and **3** are assigned to N–H stretch of N,N-diethylethylenediamine and *o*-toluidine, respectively. UV–vis [DMSO, λ_{max} (nm)] for HL_1 and the three complexes are 250.

3.3. *Inhibitory activity against jack bean urease*

The abilities of the ligands, Cu^{2+}, and complexes to inhibit urease were studied by the IC_{50} values of the material tested against *jack bean* urease according to the literature phenol-red method. The results are summarized in table 4. The IC_{50} value of the ligand and the Cu^{2+} are >10 μM. Under the same conditions, **1–3** show much stronger inhibitory activity against *jack bean* urease with an IC_{50} value of 6.8, 5.5, and 3.5 μM respectively, with the acetohydroxamic acid (IC_{50} = 7.5 μM) as a standard reference against urease.

4. Conclusion

The present study reports the synthesis, structures, and urease inhibitory activities of three copper(II) complexes with protocatechuic acid ligands. Complexes **1–3** exhibit stronger urease inhibitory activities than their parent ligands and metal ion and **3** with N,N-diethylethylenediamine co-ligand exhibited higher activity than **1** and **2** with toluidine and H_2O as co-ligands. The results indicate that the inhibitory efficiency of the complex towards urease may be influenced by the transition metal and ligands, and the inhibitory activity probably is due to strong Lewis acid properties of copper ions and the ligands strengthen the inhibitory activity of the complexes. The results are in accord with those reported previously, where some Cu(II) complexes have stronger urease inhibitory activities to urease than their parent ligands and metal ion, with IC_{50} ranging from 1 to 50 μM [15, 28, 35–39]. Compared with the data reported before, the complexes reported in this study exhibit fairly strong inhibitory activity to urease and may be used as urease inhibitors. Detailed investigations are continuing to study the inhibitory mechanism.

Supplementary material

Crystallographic data for the structural analysis has been deposited with the Cambridge Crystallographic Data Center (CCDC-925293 for **1**, CCDC-925294 for **2**, and CCDC-925295 for **3**). Copy of this information can be obtained free of charge from The Director, CCDC, 12 Union Road, Cambridge CB2 1EZ, UK (Fax: (+44) 1223-336033; E-mail: deposit@ccdc.cam.ac.uk or www: http://www.ccdc.cam.ac.uk).

Funding

We thank the financial support from National Natural Science Foundation of China [grant number 31200090]; Scientific Research Foundation for Returned Scholars, Ministry of Education of China and China Postdoctoral Science Foundation National [grant number 1302006A].

Supplemental data

Supplemental data for this article can be accessed here. [http://dx.doi.org/10.1080/00958972.2014.910597]

References

[1] H.L.T. Mobley, R.P. Hausinger. *Microbiol. Rev.*, **53**, 85 (1989).
[2] H.L.T. Mobley, M.D. Island, R.P. Hausinger. *Microbiol. Rev.*, **59**, 451 (1995).
[3] L.E. Zonia, N.E. Stebbins, J.C. Polacco. *Plant Physiol.*, **107**, 1097 (1995).
[4] C.M. Collins, S.E.F. D'Orazio. *Mol. Microbiol.*, **9**, 907 (1993).
[5] C. Montecucco, R. Rappuoli. *Nat. Rev. Mol. Cell Biol.*, **2**, 457 (2001).
[6] W. Zhengping, O.V. Cleemput, P. Demeyer, L. Baert. *Biol. Fertil. Soils*, **11**, 41 (1991).
[7] B. Krajewska. *J. Mol. Catal. B: Enzym.*, **59**, 9 (2009).
[8] Z. Amtul, A.U. Rahman, R.A. Siddiqui, M.I. Choudhary. *Curr. Med. Chem.*, **9**, 1323 (2002).
[9] W. Zaborska, M. Kot, K. Superata. *J. Enzym. Inhib. Med. Chem.*, **17**, 247 (2002).
[10] M.A. Pearson, L.O. Michel, R.P. Hausinger, P.A. Karplus. *Biochemistry*, **36**, 8164 (1997).
[11] W. Zaborska, B. Krajewska, Z. Olech. *J. Enzym. Inhib. Med. Chem.*, **19**, 65 (2004).
[12] W. Zaborska, B. Krajewska, M. Leszko, Z. Olech. *J. Mol. Catal. B: Enzym.*, **13**, 103 (2001).
[13] Y.G. Li, D.H. Shi, H.L. Zhu, H. Yan, S.W. Ng. *Inorg. Chim. Acta*, **360**, 2881 (2007).
[14] D.H. Shi, Z.L. You, C. Xu, Q. Zhang, H.L. Zhu. *Inorg. Chem. Commun.*, **10**, 404 (2007).
[15] Y.M. Cui, Y.G. Li, Y.J. Cai, W. Chen, H.L. Zhu. *J. Coord. Chem.*, **64**, 610 (2011).
[16] W. Chen, Y.G. Li, Y.M. Cui, X. Zhang, H.L. Zhu, Q.F. Zeng. *Eur. J. Med. Chem.*, **45**, 4473 (2010).
[17] Z.L. You, X. Han, G.N. Zhang. *Z. Anorg. Allg. Chem.*, **634**, 142 (2008).
[18] R.H. Liu. *J. Nutr.*, **134**, 3479S (2004).
[19] Z. Sroka, W. Cisowski. *Food Chem. Toxicol.*, **41**, 753 (2003).
[20] T. Tanaka, T. Tanaka. *J. Exp. Clin. Med.*, **3**, 27 (2011).
[21] V. Aletras, N. Hadjiliadis, D. Stabaki, A. Karaliota, M. Kamariotaki, I. Butler, J.C. Plakatouras. *Polyhedron*, **16**, 1399 (1997).
[22] S.W. Jin, D.Q. Wang. *Z. Anorg. Allg. Chem.*, **637**, 618 (2011).
[23] Y. Harrak, G. Rosell, G. Daidone. *Bioorg. Med. Chem.*, **15**, 4876 (2007).
[24] I.Y. Titov, I.K. Sagamanova, R.T. Gritsenko, I.B. Karmanova, O.P. Atamanenko, M.N. Semenova, V.V. Semenov. *Bioorg. Med. Chem. Lett.*, **21**, 1578 (2011).
[25] G.M. Sheldrick. *SADABS, Program for Empirical Absorption Correction of Area Detector*, University of Göttingen, Germany (1996).
[26] G.M. Sheldrick. *SHELXTL V5.1. Software Reference Manual*, Bruker AXS Inc., Madison, WI, USA (1997).
[27] T. Tanaka, M. Kawase, S. Tani. *Life Sci.*, **73**, 2985 (2003).
[28] C.Y. Wang. *J. Coord. Chem.*, **62**, 2860 (2009).

[29] M. Yamanaka, H. Uekusa, S. Ohba, Y. Saito, S. Iwata, M. Kato, T. Tokii, Y. Muto, O.W. Steward. *Acta Cryst. Sect. B*, **47**, 344 (1991).
[30] E.J. O'Reilly, G. Smith, C.H.L. Kennard, T.C.W. Mak, W.H. Yip. *Inorg. Chim. Acta*, **83**, L63 (1984).
[31] G. Smith, C.H.L. Kennard, H.L. Colin, K.A. Byriel. *Polyhedron*, **10**, 873 (1991).
[32] O.W. Steward, M. Kato, S.C. Chang, M. Sax, C.H. Chang, C.F. Jury, Y. Muto, T. Tokii, T. Taura, J.F. Pletcher, C. Yoo. *Bull. Chem. Soc. Jpn.*, **64**, 3046 (1991).
[33] A.W. Addison, T.N. Rao, J. Reedijk, J.V. Rijn, G.C. Verschoor. *J. Chem. Soc., Dalton Trans.*, 1350 (1984).
[34] F. Valach, M. Tokarc, T. Maris, D.J. Watkin, C.K. Prout. *J. Org. Chem.*, **622**, 166 (2001).
[35] Y.M. Cui, X.W. Dong, Y.G. Li, Z.W. Li, W. Chen. *Eur. J. Med. Chem.*, **58**, 323 (2012).
[36] X.W. Dong, Y.G. Li, Z.W. Li, Y.M. Cui, H.L. Zhu. *J. Inorg. Biochem.*, **108**, 22 (2012).
[37] C.Y. Wang, J.Y. Ye, C.Y. Lv, W.Z. Lan, J.B. Zhou. *J. Coord. Chem.*, **62**, 2164 (2009).
[38] H. Zhu, Z.Z. Wang, B. Qi, T. Huang, H.L. Zhu. *J. Coord. Chem.*, **66**, 2980 (2013).
[39] Z.M. Yang, H. Zhu, J. Sun, S.S. Qian, M.N. Cai, H.L. Zhu. *J. Coord. Chem.*, **66**, 2736 (2013).